Structural determinants in a library of low molecular weight gelators

Kyle L. Morris,[a,b] Lin Chen,[c] Alison Rodger,[b] Dave J. Adams[c] and Louise C. Serpell[a*]

Supplementary Information

The supplementary data tabulates the spectroscopic biophysical and structural data collected on gelated dipeptides from FTIR (Table S1), CD (Table S2) and fXRD (Table S3). Table S2 tabulates the Gaussian peak fitting for the CD spectra and compares the couplet x-intercept (mid-point – theoretical absorbance maxima for fitted couplet) to the experimentally measured absorbance maxima.

The CD spectra for the gelating dipeptides increase in intensity over the time course of gelation as shown in Figure S1. Absolute signal intensities were found to vary between experiments on the same system, although the sign of the peaks was found to be reproducible. This may be attributable to varying amounts of helical species (left or right) affecting the intensities of the exciton-dominated spectra. Nevertheless, the consistent sign of the peaks indicates reproducible dominance of the helical species described in the `main text. The spectra of 2-Nap AV was found to arise only after overnight incubation and CN-Nap AA did not develop any signal detectable above that of GdL. An additional couplet was observed for CN-Nap-AV with negative and positive peaks at 243 and 226 nm respectively. This couplet was not observed after overnight incubation but is used in subsequent deconvolutions. Gaussian fitting of the transitions giving rise to the CD spectra are deconvoluted and shown in Figure S2. The sign of the fitted peaks around the naphthalene absorbance maxima previously identified was used to assign naphthalene chiral assembly handedness. A long wavelength negative to short wavelength positive component indicates a left-handed and vice versa for right-handed assemblies.[1]

The indication of the close association of naphthalene groups into chiral assemblies is further indicated by the hypochromic shifting of the naphthalene absorbance maxima. Absorbance maxima may be derived from HT[V] data collected by CD measurements as shown in Figure S3. The net hypochromic shifting of naphthalene absorbance maxima is then revealed over the course of self-assembly and gelation in Figure S4.

The spectroscopic data was collected in the hydrated state whereas the structural fXRD data collected in the dried state. Figure S5 demonstrates that the diffraction signals arising from the dipeptide structure are preserved in the hydrated state. Each system exhibits strong diffraction from water at ~3 Å and the reflections arising from the structure of the dipeptide are identical to those in the dried state (see Figure 4) indicating the structure of the self-assemblies is the same in the hydrated and dried state.

Table S1. The FTIR peaks exhibited by each system in the self-assembled gel phase between 1700 – 1600 cm^{-1}. *Indicates broad overlapping peaks

System	Peak 1 / cm^{-1}	Peak 2 / cm^{-1}	Peak 3 / cm^{-1}	Peak 4 / cm^{-1}
H-Nap-AA	1712	1644	1629	1666*
H-Nap-AV	1724	1651	1629	
Br-Nap-AA	1735	1652	1633	
Br-Nap-AV	1721	1645	1628	1680*
CN-Nap-AA	1713		1627	1664
CN-Nap-AV	1734	1648	1626	

Table S2. Exciton couplets established from spectra deconvolution

System	High-energy couplet (nm)	Sign	Low-energy couplet (nm)	Sign	Helicity	Couplet mid-point (nm)	Absorbance peak (nm)
H-Nap-AA	212.4	-	218.8	+	R	215.6	220.2
H-Nap-AA	197.5	+	205.8	-	L	201.7	201.1
H-Nap-AV	219.4	+	238.8	-	L	229.1	224.0
H-Nap-AV	196.2	+	206.0	-	L	201.1	200.7
Br-Nap-AA	222.6	-	246.2	+	R	234.4	226.0
Br-Nap-AA	206.5	+	208.3	-	L	207.4	201.0
Br-Nap-AV	218.7	+	238.4	-	L	228.5	223.3
Br-Nap-AV	199.1	+	213.3	-	L	206.2	~190
CN-Nap-AA	-		-		-	-	-
CN-Nap-AA	-		-		-	-	-
CN-Nap-AV	234.3	+	236.9	-	L	235.6	229.1
CN-Nap-AV	199.9	+	207.4	-	L	203.6	~207

Table S3. The position, axial alignment and relative intensity of the equatorial and meridional reflections pertaining to the structure of the aliphatic di-peptides. The axial alignment of the reflections exhibited by CN-AA are concluded from comparison to other patterns and relative signal positions.

***Reflections near the backstop and thus partially occluded were measured manually, in these cases relative intensity was not measured. [+]Where reflection axis is not apparent due to radial averaging assignment was made by comparison to reflections from other patterns.**

H-Nap-AA

Peak resolution (Å)	Relative intensity	Axis
29	*	E
19.61	0.58	E
14.16	**0.61**	**E**
-	-	-
5.79	**1.00**	**E**
4.68	**0.80**	**M**

H-Nap-AV

Peak resolution (Å)	Relative intensity	Axis
-	-	-
-	-	-
14.37	**0.97**	**E**
6.41	0.73	E
5.55	**0.73**	**E**
4.70	**1.00**	**M**

Br-Nap-AA

Peak resolution (Å)	Relative intensity	Axis
29	*	E
-	-	-
-	-	-
10.23	0.48	E
-	-	-
-	-	-
-	-	-
5.30	**1.00**	**E**
-	-	-
4.58	0.62	E
3.94	0.63	E
-	-	-
4.51	**0.99**	**M**
-	-	-
4.09	0.92	M
3.66	0.64	M
3.43	0.60	M

Br-Nap-AV

Peak resolution (Å)	Relative intensity	Axis
29	*	E
16.95	0.66	E
13.20	0.58	E
10.95	0.50	E
8.99	0.51	E
7.51	0.61	E
6.61	0.69	E
5.54	**0.83**	**E**
-	-	-
-	-	-
-	-	-
-	-	-
4.56	**1.00**	**M**
-	-	-
-	-	-
3.79	0.80	OM
-	-	-

CN-Nap-AA

Peak resolution (Å)	Relative intensity	Axis
-	-	-
12.96	0.76	E^+
10.93	0.77	E^+
9.49	0.83	E^+
6.60	**0.95**	**E^+**
5.82	0.87	-
4.65	**1.00**	**M^+**
4.50	0.85	M^+
4.07	0.94	-
3.55	0.89	-

CN-Nap-AV

Peak resolution (Å)	Relative intensity	Axis
15.97	0.66	E
12.46	0.69	E
10.86	*	E
9.63	0.74	E
6.23	**0.97**	**E**
-	-	-
4.69	*	**M**
4.53	1.00	M
-	-	-
-	-	-

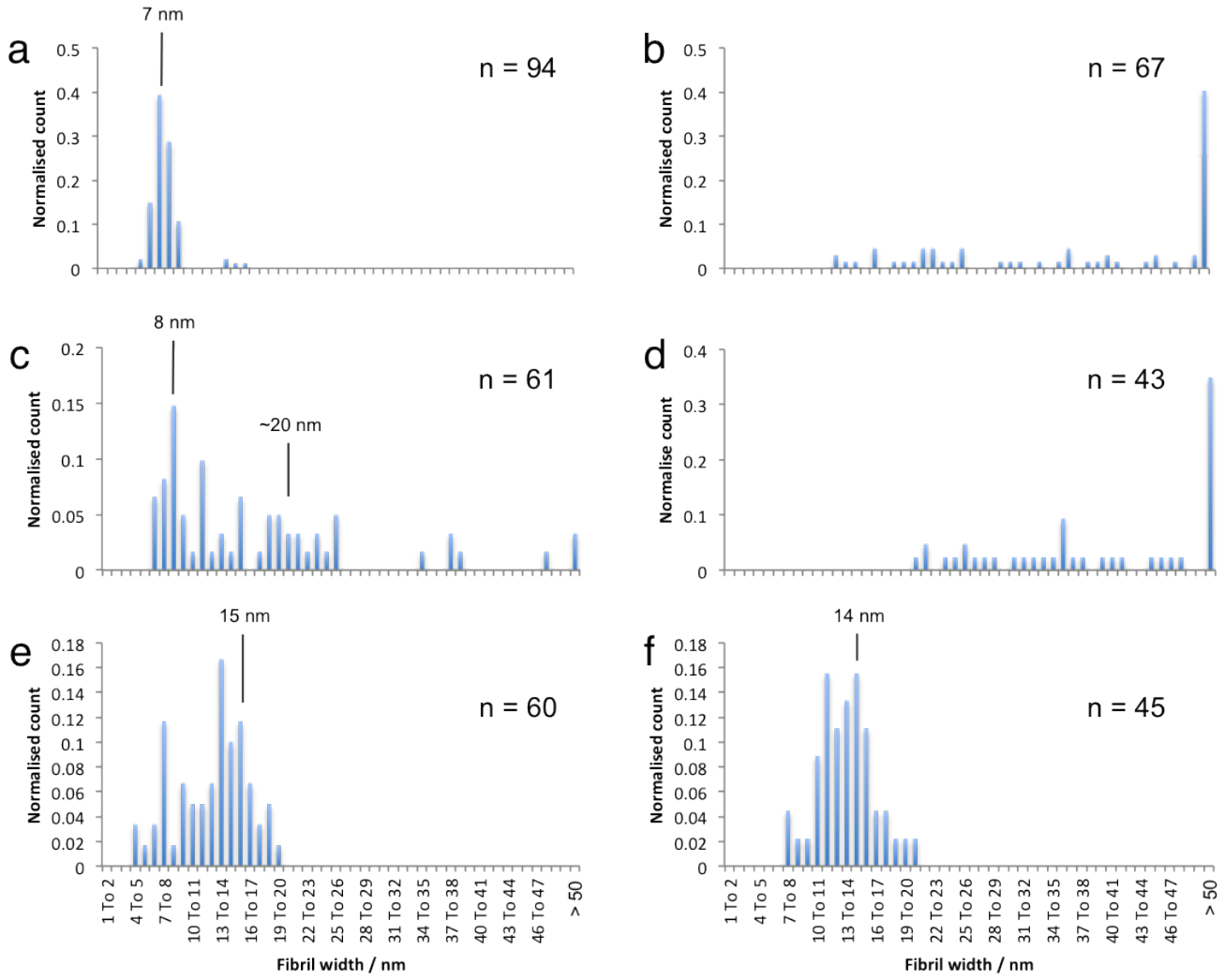

Figure S1. Analysis of fibril morphology by characterisation of fibril width. (a) H-Nap-AA, (b) H-Nap-AV, (c) Br-Nap-AA, (d) Br-Nap-AV, (e) CN-Nap-AA and (f) CN-Nap-AV. Unbiased measurements were made on the micrographs (Figure 2) and the distribution of sizes plotted by histogram, sizes corresponding to predominantly observed fibril widths are highlighted.

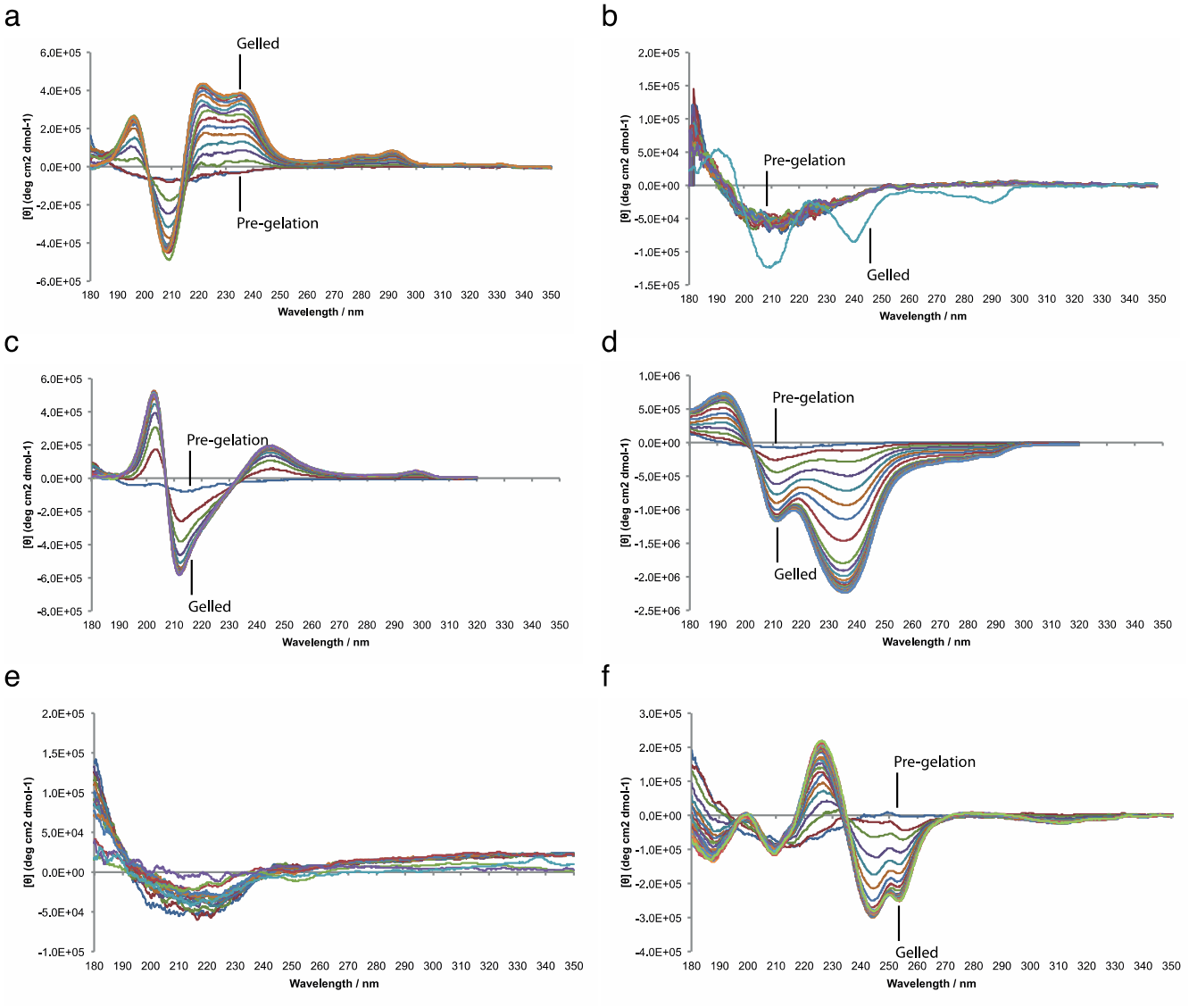

Figure S2. The development of circular dichroism signals over the course of *in situ* self-assembly and gelation. All signals increase from the background spectra to the characteristic peak profiles shown in the main text (Figure 3). (a) H-Nap-AA, (b) H-Nap-AV, (c) Br-Nap-AA, (d) Br-Nap-AV, (e) CN-Nap-AA, (f) CN-Nap-AV. Data collected on a Jasco J-715 spectropolarimeter at 21 °C in a 0.01 mm pathlength.

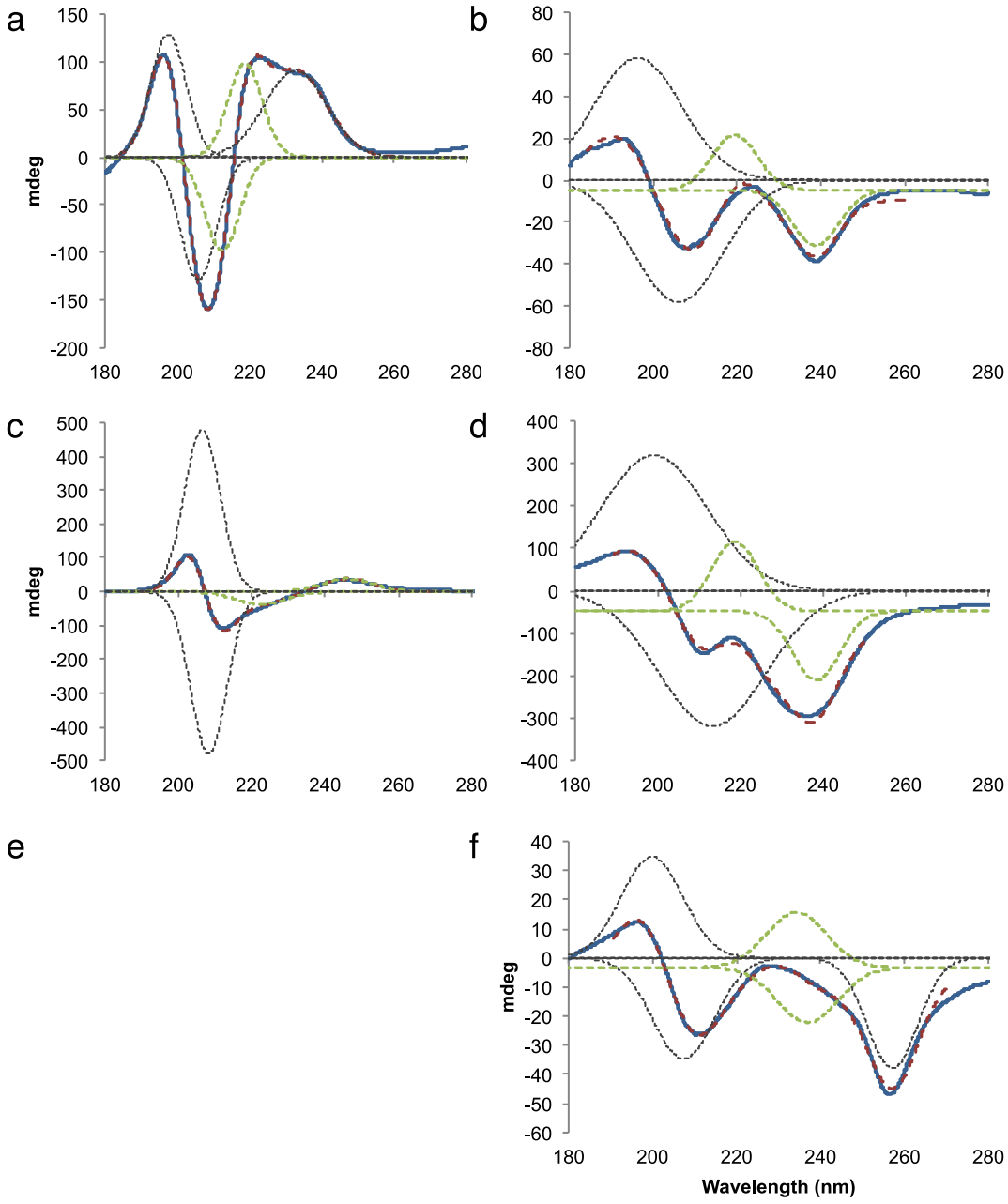

Figure S3. Spectra of Figure S1 collected at completion of gelation and deconvolved to reveal the Gaussian components of each CD spectra. The (blue solid) experimental data, (dashed red) fitted data, (grey dashed) fitted Gaussian components and (green dashed) exciton couplets modeled to arise from interactions of the naphthalene groups are shown. Minimised sum of square fitting was performed between approximately 190 – 260 nm. (a) H-Nap-AA, (b) H-Nap-AV, (c) Br-Nap-AA, (d) Br-Nap-AV, (e) Data deconvolution not possible, (f) CN-Nap-AV.

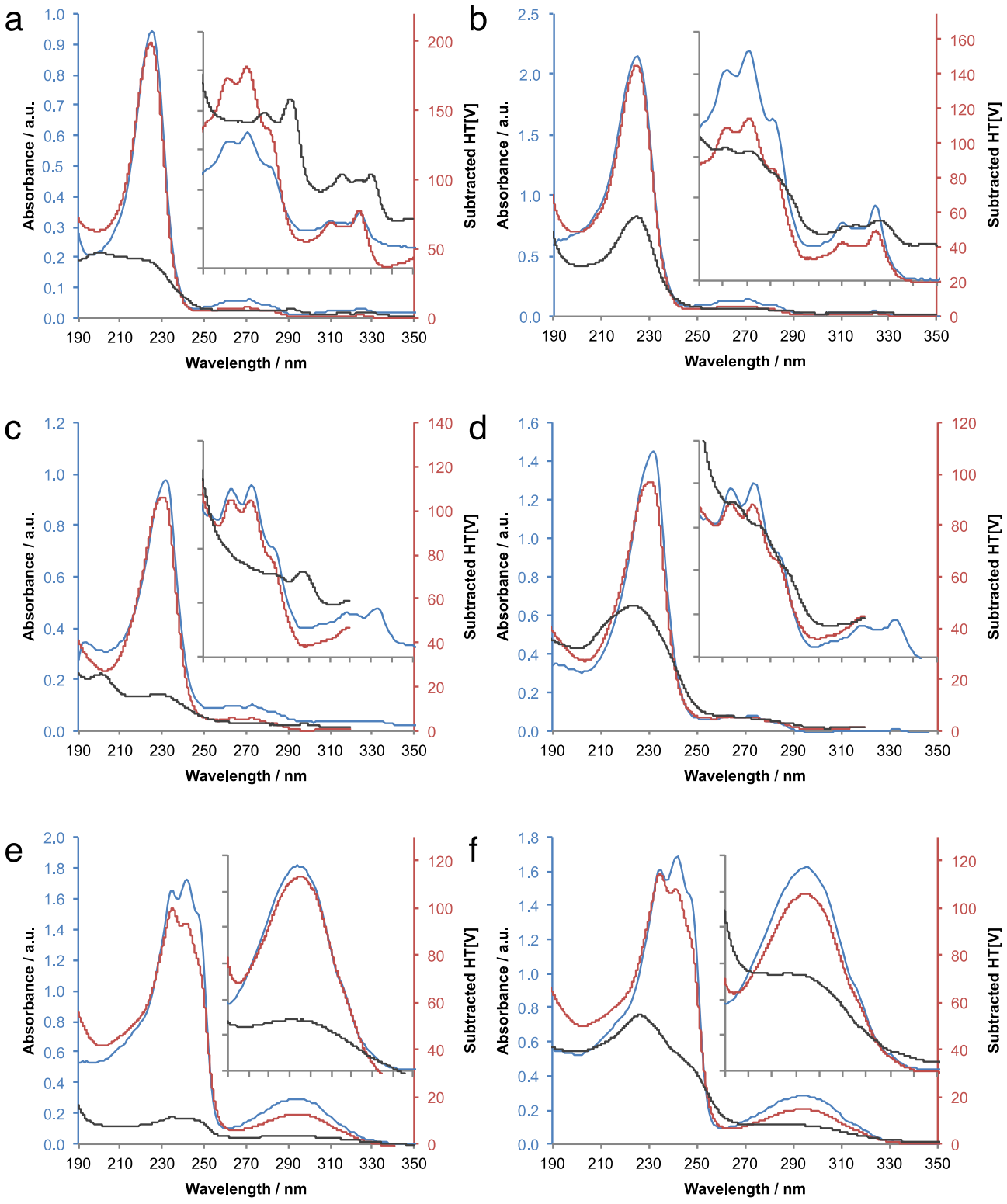

Figure S4. Absorption data for the dipeptide systems including (blue) UV/Vis absorbance and (red) HT[V] of stock before gelation compared to (black) HT[V] exhibited by gelled solutions. HT[V] values have been buffer subtracted to reveal the absorbance spectrum from the sample. The overlay of the UV/Vis and HT[V] data demonstrates the validity of subtracted HT[V] data as an absorbance measurement. UV/Vis data collected on a Shimadzu UV/Vis UV2400PC in a 1 cm pathlength at room temperature. HT[V] data collected on a Jasco J-715 spectropolarimeter at 21 °C in a 0.01 mm pathlength. (a) H-Nap-AA, (b) H-Nap-AV, (c) Br-Nap-AA, (d) Br-Nap-AV, (e) CN-Nap-AA, (f) CN-Nap-AV

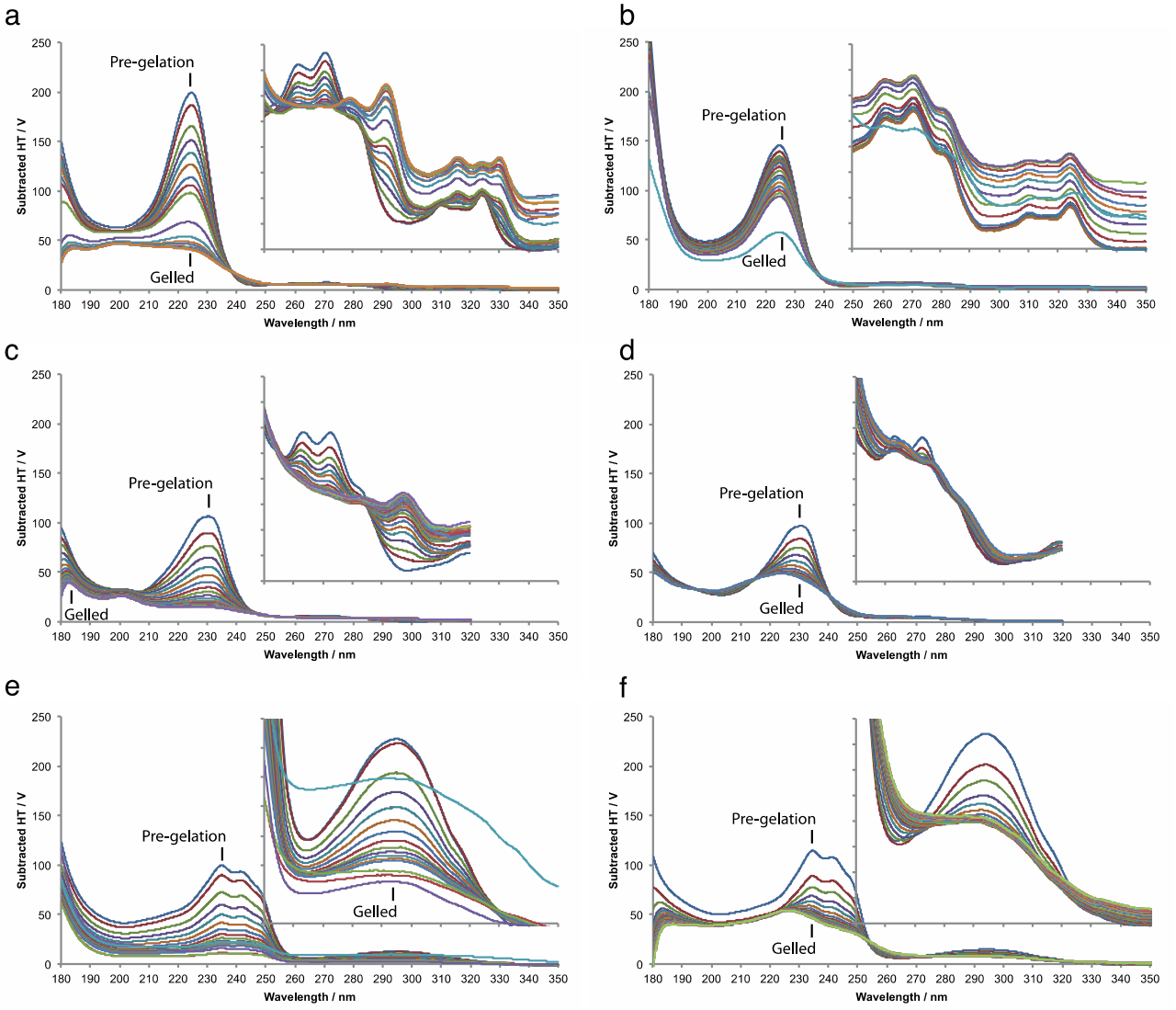

Figure S5. HT[V] data of the dipeptide systems with HT[V] data of the background solvent subtracted, data are shown over the course of gelation. Inserts show expanded spectra for the 250 – 350 nm region. Data collected on a Jasco J-715 spectropolarimeter at 21 °C in a 0.01 mm pathlength. (a) H-Nap-AA, (b) H-Nap-AV, (c) Br-Nap-AA, (d) Br-Nap-AV, (e) CN-Nap-AA, (f) CN-Nap-AV

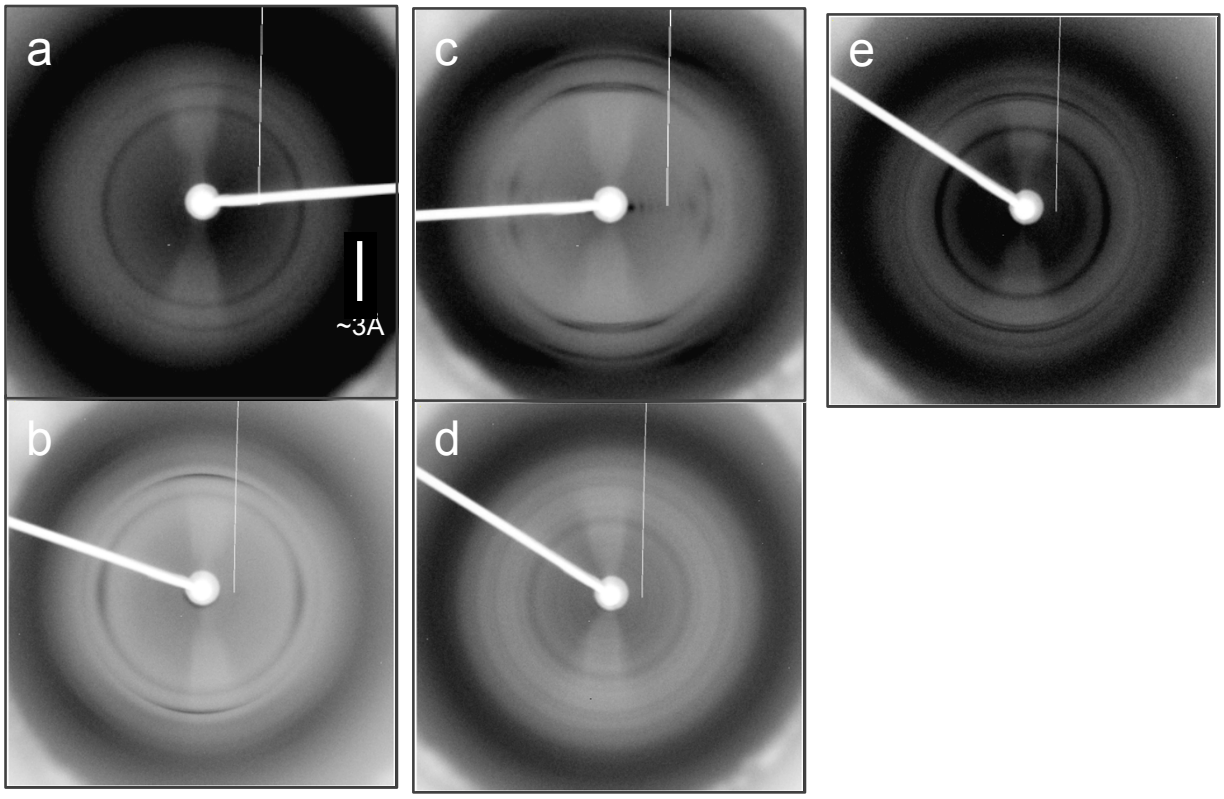

Figure S6. X-ray fibre diffraction data of the library (a) H-Nap-AA, (b) Br-Nap-AA, (c) Br-Nap-AV, (d) CN-Nap-AA, (e) CN-Nap-AV in the semi-hydrated states.

REFERENCES

(1) Rodger, A.; Norden, B. *Circular Chroism & Linear Dichroism*; OUP Oxford, 1997.